PHYSICAL REVIEW D VOLUME 21, NUMBER 8 15 APRIL 1980

Surfaces of infinite red-shift around a uniformly accelerating and rotating particle

Hamid Farhoosh and Robert L. Zimmerman
Department of Physics and Institute of Theoretical Science, University of Oregon, Eugene, Oregon 97403
(Received 9 August 1979; revised manuscript received 17 December 1979)

The structure of the surfaces of infinite red-shift that are formed about an accelerating Kerr-type particle is studied. It is shown that for nonzero acceleration and rotation there exist three relevant surfaces of infinite red-shift. One of these surfaces is analogous to the Schwarzschild surface and is mainly a consequence of the mass. The acceleration causes this surface to expand in the forward direction and contract in the backward direction. In addition, the rotation causes the Schwarzschild surface to contract both in the forward and backward directions. The second surface is mainly due to the acceleration and is called the Rindler surface. It has a shape similar to a parabola of revolution. As the acceleration increases, the Rindler surface moves inward, approaching the Schwarzschild surface. Rotation causes the Rindler surface to contract slightly in the equatorial plane. As the acceleration increases to a critical value the Rindler and the Schwarzschild surfaces coincide on the equatorial plane. As the acceleration is increased further, the points of coincidence spread towards the poles. The third surface is produced mainly by the rotation and is a shape similar to the interior Kerr surface. This surface is called the Kerr surface. By increasing the rotation this surface expands in the polar regions, approaching the Schwarzschild surface. Acceleration causes this surface to distort and become elongated in the forward direction and contracted in the backward direction.

I. INTRODUCTION

The stationary c metric is a vacuum type-D solution of the Einstein field equations. This solution represents the gravitational field of a uniformly accelerating Kerr-type particle. It represents the generalization of the static c-metric solution to include rotation of the particle. Although the static c metric was discovered in 1918, the physical interpretation was unknown until 1970. The physical interpretation of the static vacuum c metric was recognized by Kinnersley and Walker[1] and studied further by Farhoosh and Zimmerman.[2,3] The generalization of the static c metric to include rotation was done by Kinnersley[4] and by Plebanski and Demianski.[5]

It is the purpose of this paper to explore the physical properties of the stationary vacuum c metric. In particular, we will investigate the shape of the surface of infinite red-shift that are formed about a rotating and accelerating particle.

The Schwarzschild surface is a well-known example of a surface of infinite red-shift. Since the metric is static, it has a hypersurface orthogonal timelike Killing vector $\xi^{\mu}_{(t)}$. Relative to this vector there exists a class of static observers whose four-velocity vectors are defined by

$$\nu^{\mu}=\xi^{\mu}_{(t)}/(+\xi^{\mu}_{(t)}\xi^{\mu}_{(t)})^{1/2}\,. \tag{1.1}$$

It follows that the red-shift between a static observer and source is given by

$$\frac{\nu_0}{\nu_s}=\frac{[+(\xi^{\mu}_{(t)}\xi^{\mu}_{(t)})_s]^{1/2}}{[+(\xi^{\mu}_{(t)}\xi^{\mu}_{(t)})_0]^{1/2}}\,. \tag{1.2}$$

The surfaces of infinite red-shift are defined to be those surfaces where the norm of the timelike Killing vector vanishes.

Farhoosh and Zimmerman[3] have studied the shapes of the surfaces of infinite red-shift for a Schwarzschild-type particle undergoing uniform acceleration. That is, they studied the properties of those surfaces in the static c metric that were defined by the vanishing of the norm of the timelike Killing vector. In both the case of the Schwarzschild and static c-metric solutions the surfaces of initinite red-shift are also null surfaces. These surfaces are Killing horizons.

For the static vacuum c metric there exist two Killing horizons or surfaces of infinite red-shift as opposed to the one for the Schwarzschild metric. One is analogous to the familiar Schwarzschild surface which is deformed by the acceleration. The acceleration causes this Killing horizon to elongate in the forward direction and contract in the backward direction. The second Killing horizon is due to the acceleration of the particle. It is a parabola of revolution with its opening in the forward direction and surrounding the Schwarzschild-type surface. This surface is called the Rindler surface. The reason for the existence of this surface is obvious. Photons that have been sent from the Rindler surface towards the accelerating particle will never reach the particle. During the flight time of the photon, the particle's velocity will have reached the velocity of light. The surface is open in the forward direction because the particle is moving in that direction and will receive all the photons.

By increasing the acceleration, the Schwarzschild-type surface becomes more deformed, ex-

panding in the forward direction and contracting in the backward direction, in agreement with what would have been expected from the principle of equivalence. However, when the acceleration increases to the value $A=1/\sqrt{54}m$ (m is the mass and A is the acceleration of the particle), the Schwarzschild surface reaches its maximum contraction in the backward direction and as the acceleration increases beyond this value, the surface in the backward direction expands outward again. The expansion of this surface appears to be a violation of the principle of equivalence. On the other hand, as the acceleration increases, the Rindler surface moves inward and at some critical value given by $A=1/\sqrt{27}m$, the Rindler and the Schwarzschild-type surfaces coincide at all points on their surfaces simultaneously and produce a naked singularity at the position of the particle.

The properties of the surfaces of infinite red-shift change considerably when rotation is included. The timelike Killing vector $\xi^{\mu}_{(t)}$ is no longer hypersurface orthogonal. Relative to this timelike Killing vector, we define a class of stationary observers whose four-velocity vectors are defined by

$$v^{\mu}=\xi^{\mu}_{(t)}/(+\xi^{\mu}_{(t)}\xi^{\mu}_{(t)})^{1/2}. \tag{1.3}$$

The surfaces of infinite red-shift are again those surfaces where the norm of the timelike Killing vector vanishes.

For the Kerr metric, the region between the surface of infinite red-shift and the null surface is called the ergosphere. The ergosphere is a region in which special trajectories may pierce the surface of infinite red-shift, entering the ergosphere, and then escape back through the surface of infinite red-shift carrying more energy to infinity than they started out with. This energy is gained at the expense of the loss of rotational energy in the Kerr line element.

A similar generalization occurs in going from the static c metric to the stationary c metric as in going from the Schwarzschild metric to the Kerr metric. That is, the surface of infinite red-shift are no longer null surfaces. Again, an ergosphere is formed beneath the surface of infinite red-shift. Now trajectories that plunge through the surface of infinite red-shift can extract energy not only due to the rotation but also the acceleration. The class of stationary observers are stationary relative to the particle. Since the particle is undergoing uniform rectilinear acceleration, these stationary observers are actually uniformly accelerating observers relative to the inertial space.

The purpose of this article is to study the effects of acceleration on the surfaces of infinite red-shift that exist about a Kerr-type particle. In Sec. II we will discuss the line element for the stationary c metric and give a physical meaning to the coordinates. In Sec. III the shapes of the surfaces of infinite red-shift are investigated. It is shown in this section that with rotation and acceleration there exist three relevant surfaces of infinite red-shift. One is the familiar Schwarzschild surface which is due to the mass of the particle. Acceleration causes this surface to distort and become elongated in the forward direction and contracted in the backward direction. Rotation, on the other hand, causes this surface to contract along the poles.

The second surface is the Rindler surface which has a similar structure to the nonrotating case and is mainly due to the acceleration and is distorted by the mass and the rotation of the particle. Rotation causes this surface to slightly contract in the equatorial region.

The third surface is due to rotation and it is analogous to the interior Kerr surface which is distorted by the acceleration. Acceleration causes this surface to slightly expand in the forward direction and shrink in the backward direction. The effects produced by the increase of the acceleration and the rotation are also discussed in this section.

As was the case for the static c metric, we also observe an apparent violation of the principle of equivalence for the Schwarzschild-type surface. For sufficiently large accelerations, the Schwarzschild-type surface expands in the backward direction, which appears to be contrary to the principle of equivalence.

II. METRIC

The stationary vacuum c metric which represents the gravitational field of a uniformly accelerating and rotating particle can be expressed as[5]

$$ds^2=\frac{1}{(\xi+\eta)^2}\left[\frac{Q}{1+(\xi\eta)^2}(d\tau-\xi^2d\sigma)^2-\frac{1+(\xi\eta)^2}{Q}d\eta^2-\frac{P}{1+(\xi\eta)^2}(d\sigma+\eta^2d\tau)^2-\frac{1+(\xi\eta)^2}{P}d\xi^2\right], \tag{2.1}$$

where

$$P=P(\xi)=\gamma_0-\epsilon_0\xi^2+2m_0\xi^3-\gamma_0\xi^4, \tag{2.2a}$$

$$Q = Q(\eta) = -\gamma_0 + \epsilon_0\eta^2 + 2m_0\eta^3 + \gamma_0\eta^4 , \tag{2.2b}$$

and

$$\gamma_0 \equiv \frac{1}{a^2+b^2}, \quad \epsilon_0 \equiv -\frac{1}{ab}\,\frac{a^2-b^2}{a^2+b^2} . \tag{2.3}$$

The coordinates in Eq. (2.1) are mathematically convenient; however, their physical interpretation is obscure. We would like to express Eq. (2.1) in a coordinate system where the physical meaning of the coordinates becomes more apparent as are the Boyer-Lindquist coordinates for the Kerr metric. It is shown in the Appendix that the line element (2.1) can be transformed to

$$ds^2 = \frac{1}{A^2(p+q)^2}\{A^2W^{-1}(F - a^2A^2q^4G)dt^2 - 2aA^2W^{-1}[F(1-p^2) - Gq^2(1+a^2A^2q^2)]dt\,d\omega - WF^{-1}dq^2 - WG^{-1}dp^2 - W^{-1}[G(1+a^2A^2q^2)^2 - a^2A^2F(1-p^2)^2]d\omega^2\}, \tag{2.4}$$

where

$$G = G(p) = \gamma - \epsilon p^2 - 2Amp^3 - a^2A^2\gamma p^4 , \tag{2.5a}$$

$$F = F(q) = -\gamma + \epsilon q^2 - 2Amq^3 + a^2A^2\gamma q^4 , \tag{2.5b}$$

and

$$W \equiv 1 + a^2A^2p^2q^2 , \tag{2.6}$$

$$\gamma \equiv \frac{1}{1+a^2A^2} , \tag{2.7}$$

$$\epsilon \equiv \frac{1-a^2A^2}{1+a^2A^2} . \tag{2.8}$$

In these equations m is the mass, A is the acceleration, a is the rotation of the particle, t is the time coordinate, and ω, p, and q are the spatial coordinates. In the absence of rotation, the line element (2.4) reduces to the nonrotating line element as expressed by the static c metric.[6] Comparing (2.5) with Eq. (2.2) in Ref. 3 one can see that rotation introduces a fourth-order term in the polynomials $G(p)$ and $F(q)$ raising them to quartic functions. Figure 1 shows the behavior of the quartic function $G(p)$ under the change of rotation and acceleration. In analogy to the nonrotating case, the roots of the function $G(p)$ determine the range of the p coordinate and are denoted by p_0 and p_π in Fig. 1.

The line element (2.4) can be transformed to a uniformly accelerating spherical-like coordinate system by letting

$$r = 1/A(p+q) , \tag{2.9a}$$

$$G(p) = \gamma \sin^2\theta , \tag{2.9b}$$

$$\omega = \phi . \tag{2.9c}$$

The line element (2.4) in this case transforms to

$$ds^2 = A^2r^2W^{-1}(F - a^2A^2\gamma \sin^2\theta q^4)dt^2 - 2aA^2r^2W^{-1}[F(1-p^2) - \gamma \sin^2\theta q^2(1+a^2A^2q^2)]dt\,d\phi - \frac{W}{A^2r^2F}dr^2 - \frac{2W}{AF}dr\,dp - r^2W\left(\frac{1}{F} + \frac{1}{\gamma \sin^2\theta}\right)dp^2 - W^{-1}r^2[\gamma \sin^2\theta(1+a^2A^2q^2)^2 - a^2A^2F(1-p^2)^2]d\phi^2 , \tag{2.10}$$

where p and q are related to the spherical coordinates r and θ by Eqs. (2.9).

Equation (2.9b) is a mapping from the p variable to the θ variable and in general it has four solutions. Because of the mathematical complexities involved in the solutions of quartic equations, a better grasp of the problem can be obtained by the method of numerical analysis. In order to make the mapping between the p and the θ variables unique, one has to make a proper identification between the two variables. A similar situation arises in the nonrotating case. In analogy of the nonrotating case we pick that solution of Eq. (2.9b) which, at $\theta = 0$, becomes $p(\theta = 0) = p_0$ and at $\theta = \pi$ it becomes $p(\theta = \pi) = p_\pi$ (cf. Fig. 1). This mapping between the p and the θ variables is numerically tabulated in Table I for different values of a and A.

The meaning of the coordinates (t, r, θ, ϕ) and parameters A, a, and m becomes apparent by considering various limiting cases. In the limit that $a \to 0$ the line element in (2.10) reduces to the line element (2.23) of Ref. 3. In this limit, the (t, r, θ, ϕ) coordinates represent a uniformly accelerating coordinate system "rigidly" attached to a Schwarzschild-type particle. The further reduction of $A \to 0$ causes the line element to reduce to the nonaccelerating Schwartzschild solution with the usual spherical coordinates. We see that m is the mass of the particle and A is the acceleration. If we only let $A \to 0$ in (2.10), the line element reduces to the Kerr metric in the Boyer-Lindquist coordinates. Consequently, we interpret (2.10) to be a Kerr-type particle with rotation a, acceleration A, and mass m described by a uniformly accelerating coordinate system rigidly attached to the particle.

To gain further insight into the meaning of (t, r, θ, ϕ) described by (2.10), let us consider the limit that $m \to 0$. In this limit, space-time becomes Euclidean and the metric in (2.4) reduces to

$$ds^2 = \frac{1}{A^2(p+q)^2}\left\{A^2\gamma[(q^2-1)+a^2A^2q^2(1-p^2)]dt^2 + 2aA^2\gamma(1-p^2)(1+a^2A^2q^2)dt\,d\omega - \frac{W}{\gamma(q^2-1)(1+a^2A^2q^2)}dq^2 - \frac{W}{\gamma(1-p^2)(1+a^2A^2p^2)}dp^2 - (1-p^2)(1+a^2A^2q^2)d\omega^2\right\}. \tag{2.11}$$

This is a special form of the flat-space line element written in a uniformly accelerating and rotating frame. Performing the coordinate transformation

$$\bar{\rho} = \frac{[(1-p^2)(1+a^2A^2q^2)]^{1/2}}{A(p+q)}, \tag{2.12a}$$

$$\bar{t} = \frac{[(q^2-1)(1+a^2A^2p^2)]^{1/2}}{A(p+q)}\sinh A\gamma t, \tag{2.12b}$$

$$\bar{z} = \frac{1}{A} - \frac{[(q^2-1)(1+a^2A^2p^2)]^{1/2}}{A(p+q)}\cosh A\gamma t, \tag{2.12c}$$

$$\bar{\phi} = \omega + aA^2\gamma t, \tag{2.12d}$$

the line element (2.11) reduces to

$$ds^2 = d\bar{t}^2 - d\bar{\rho}^2 - d\bar{z}^2 - \bar{\rho}^2 d\bar{\phi}^2. \tag{2.13}$$

Equation (2.13) is the familiar flat-space line element written in the nonaccelerating cylindrical coordinates.

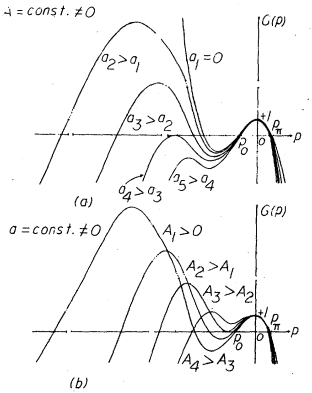

FIG. 1. The behavior of the quartic function $G(p)$ under the change of the rotation for a fixed value of acceleration (a), and its behavior under the change of the acceleration for a fixed value of rotation (b), is shown.

We conclude this section with the observation that the line element in Eq. (2.10) represents a uniformly accelerating Kerr-type particle which is accelerating along the positive $\bar{z}$ axis. The coordinate system (t, r, θ, ϕ) defined by Eq. (2.10) is a coordinate system rigidly fixed on the accelerating particle. Coordinate transformations (2.12) are the transformation equations to the $(\bar{t}, \bar{\rho}, \bar{z}, \bar{\phi})$ coordinates which constitute the nonaccelerating frame relative to the Euclidean background space.

III. SURFACES OF INFINITE RED-SHIFT

In this section we will discuss the surfaces of infinite red-shift that surrounded a uniformly accelerating Kerr-type object. In order to gain a clear insight of the problem, we first review the surfaces of infinite red-shift for the Kerr metric.

For a stationary metric we define a stationary observer to the one whose four-velocity vector satisfies Eq. (1.3). The timelike Killing vector of the Kerr metric in the Boyer-Lindquist coordinate system is

$$\xi^{\mu}_{(t)} = (1, 0, 0, 0)$$

and its norm is

$$\xi^{\mu}_{(t)}\xi^{\mu}_{(t)} = g_{00} = -(r^2 - 2mr + a^2\cos^2\theta).$$

The Killing vector becomes null on the two surfaces

$$r_0 = m + (m^2 - a^2\cos^2\theta)^{1/2},$$

$$r_i = m - (m^2 - a^2\cos^2\theta)^{1/2}.$$

Outside the outer surface r_0, we can have stationary sources and observers with four-velocities following the Killing-vector trajectories. As an observer approaches this outer surface, the dragging of the inertial frame due to the rota-

TABLE I. This table shows the mapping between the p and the θ variables for different values of rotation and acceleration. Those values of $p(\theta)$ that are distinguished by a dagger are the double roots of the equation $G(p)=\gamma \sin^2\theta$.

			$a^2 = 0.2m^2$			
	$A^2m^2 = 1/4\times 54$	$A^2m^2 = \frac{1}{54}$	$A^2m^2 = 3/2\times 54$	$A^2m^2 = \frac{1}{27}$	$A^2m^2 = 0.035\,74$	$A^2m^2 = 0.038\,20$
θ	$p(\theta)$	$p(\theta)$	$p(\theta)$	$p(\theta)$	$p(\theta)$	$p(\theta)$
0°	−1.083	−1.224	−1.343	−1.597	−1.531	−1.760†
10°	−1.065	−1.200	−1.310	−1.516	−1.471	−1.575
45°	−0.746	−0.801	−0.834	−0.870	−0.864	−0.875
90°	0	0	0	0	0	0
135°	+0.677	+0.652	+0.642	+0.634	+0.636	+0.634
180°	+0.941	+0.897	+0.879	+0.865	+0.868	+0.864
			$a^2 = 0.4m^2$			
					$A^2m^2 = 0.034\,56$	$A^2m^2 = 0.039\,50$
0°	−1.083	−1.223	−1.339	−1.555	−1.473	−1.790†
10°	−1.065	−1.199	−1.308	−1.493	−1.426	−1.601
45°	−0.746	−0.802	−0.836	−0.873	−0.863	−0.884
90°	0	0	0	0	0	0
135°	+0.677	+0.652	+0.643	+0.635	+0.637	+0.633
180°	+0.941	+0.896	+0.879	+0.866	+0.869	+0.862
			$a^2 = 0.8m^2$			
					$A^2m^2 = 0.032\,51$	$A^2m^2 = 0.042\,72$
0°	−1.083	−1.222	−1.333	−1.507	−1.408	−1.880†
10°	−1.065	−1.198	−1.303	−1.460	−1.372	−1.675
45°	−0.747	−0.804	−0.841	−0.881	−0.861	−0.909
90°	0	0	0	0	0	0
135°	+0.677	+0.653	+0.644	+0.636	+0.640	+0.632
180°	+0.941	+0.896	+0.879	+0.865	+0.872	+0.858
			$a^2 = m^2$			
					$A^2m^2 = 0.031\,61$	$A^2m^2 = 0.044\,82$
0°	−1.083	−1.221	−1.329	−1.490	−1.386	−1.950†
10°	−1.065	−1.198	−1.300	−1.448	−1.353	−1.730
45°	−0.747	−0.806	−0.843	−0.884	−0.860	−0.925
90°	0	0	0	0	0	0
135°	+0.677	+0.653	+0.644	+0.637	+0.641	+0.632
180°	+0.941	+0.896	+0.879	+0.865	+0.873	+0.855
			$a^2 = 1.043\,09m^2$			
		$A^2m^2 = 0.01$			$A^2m^2 = 0.031\,42$	$A^2m^2 = 0.045\,33$
0°	−1.083	−1.137	−1.329	−1.487	−1.382	−1.990†
10°	−1.065	−1.117	−1.300	−1.445	−1.349	−1.745
45°	−0.747	−0.772	−0.844	−0.885	−0.860	−0.929
90°	0	0	0	0	0	0
135°	+0.677	+0.665	+0.644	+0.637	+0.641	+0.632
180°	+0.941	+0.919	+0.879	+0.865	+0.873	+0.855

tion becomes more extreme. At r_0 the dragging becomes so extreme that no observer can remain at rest there relative to the distant stars. Inside this surface all observers with fixed r and θ must orbit the black hole in the same direction in which the hole rotates. The Killing vector changes from timelike to spacelike inside the r_0 surface.

If we let the rotating particle also possess acceleration, the inertial frame will not only be dragged by the rotation but also by the accelera-

tion. The surfaces of infinite red-shift that occurred in the Kerr solution become distorted by the acceleration in addition to the appearance of a third surface due to the introduction of acceleration.

To study the effect of acceleration on the surfaces of infinite red-shift that occur about a uniformly accelerating Kerr-type particle, we consider the line element in Eq. (2.10). This line element has two Killing vectors given by

$$\xi^{\mu}_{(t)} = (1,0,0,0), \tag{3.1a}$$

$$\xi^{\mu}_{(\phi)} = (0,0,0,1), \tag{3.1b}$$

whose norms are

$$\xi^{\mu}_{(t)}\xi^{\mu}_{(t)} = A^2r^2W^{-1}(F - a^2A^2\gamma\sin^2\theta q^4)$$
$$= A^2r^2W^{-1}(-\gamma + \epsilon q^2 - 2Amq^3 + a^2A^2\gamma\cos^2\theta q^4), \tag{3.2a}$$

$$\xi^{\mu}_{(\phi)}\xi^{\mu}_{(\phi)} = -r^2W^{-1}[\gamma\sin^2\theta(1 + a^2A^2q^2)^2 - a^2A^2F(1-p^2)^2]. \tag{3.2b}$$

μ runs from 0 to 3 denoting (t, r, p, ϕ), respectively. $\xi^{\mu}_{(t)}$ is the timelike Killing vector representing the time symmetry and the stationary structure of the metric. $\xi^{\mu}_{(\phi)}$ is the spacelike Killing vector and represents the axial symmetry of the solution. The surfaces of infinite red-shift are defined by setting the norm of the timelike Killing vector $\xi^{\mu}_{(t)}$ given in Eq. (3.2a) equal to zero. One possible solution is $r = 0$. This solution is not meaningful because of intrinsic singularity at the origin and will not be considered any longer. The other surfaces follow from the solution of the quartic equation

$$F - a^2A^2\gamma\sin^2\theta q^4 = -\gamma + \epsilon q^2 - 2Amq^3 + a^2A^2\gamma\cos^2\theta q^4 = 0. \tag{3.3}$$

The quartic Eq. (3.3), in general, has four roots which can either be real or nonreal depending on the value of the discriminant of the equation.[7] The discriminant of the quartic Eq. (3.3) is given by

$$\Delta = 16A^2m^2\gamma\epsilon^3\left[1 - 27\frac{A^2m^2\gamma}{\epsilon^3} + 36a^2A^2\frac{\gamma^2}{\epsilon^2}\cos^2\theta - \frac{a^2}{m^2}\gamma\epsilon\cos^2\theta\left(1 + 4a^2A^2\frac{\gamma^2}{\epsilon^2}\cos^2\theta\right)^2\right]. \tag{3.4}$$

For $\Delta > 0$ there are four real and distinct roots. For $\Delta = 0$ two of the roots are equal and for $\Delta < 0$ there are two real and two nonreal roots. Table II demonstrates different combinations of A^2m^2 and a^2/m^2 at different angles for which the discriminant vanishes.

To see the effect of acceleration on the surfaces of infinite red-shift about a rotating object let us consider the case where both a and A are small. In this case the discriminant is positive and there are four real roots. In analogy to the static c-metric solution, one of these roots occurs for negative values of r and lies outside the physical range of the radial coordinate. This case will not be considered any further. The other three roots denoted by q_R, q_S, and q_K are numerically tabulated in Table III for different values of the rotation a, acceleration A, and angle θ.

It was to be expected from the analogy with the Kerr metric and static c metric that there should exist three surfaces of infinite red-shift. From

TABLE II. This table demonstrates the numerical values of the rotation and the acceleration parameters for which the discriminant of the quartic equation $F - a^2A^2\gamma\sin^2\theta q^4 = 0$ vanishes. An asterisk in this table expresses the fact that no real value of the rotation exists in that situation to satisfy the condition $\Delta = 0$.

θ	a^2/m^2	A^2m^2
0°	* , 1.0165	0.004
10°	* , 1.0485	0.004
90°	* , ∞	0.004
180°	* , 1.0165	0.004
0°	* , 1.0431	0.01
10°	* , 1.0766	0.01
90°	* , ∞	0.01
180°	* , 1.0431	0.01
0°	* , 1.0939	0.02
10°	* , 1.1305	0.02
90°	* , ∞	0.02
180°	* , 1.0939	0.02
0°	0 , 1.2100	$\frac{1}{27}$
10°	0 , 1.2545	$\frac{1}{27}$
90°	0 , ∞	$\frac{1}{27}$
180°	0 , 1.2100	$\frac{1}{27}$
0°	0.2 , 1.2201	0.0382
10°	0.2150 , 1.2654	0.0382
90°	* , ∞	0.0382
180°	0.2 , 1.2201	0.0382
0°	0.8 , 1.2870	0.0427
10°	0.8515 , 1.3127	0.0427
90°	* , ∞	0.0427
180°	0.8 , 1.2870	0.0427
0°	1 , 1.2874	0.0448
10°	1 , 1.3300	0.0442
90°	1 , ∞	0.0316
180°	1 , 1.2874	0.0448
0°	1.0165 , 1.2897	0.0450
10°	1.0781 , 1.3407	0.0450
90°	* , ∞	0.0450
180°	1.0165 , 1.2987	0.0450

TABLE III. In this table the three relevant values of q, for which the norm of the timelike Killing vector vanishes, are evaluated for different values of rotation and different values of acceleration. Sections of this table that are marked by a dagger correspond to the case where there exists a double root at $\theta = 90°$ angle or the equatorial plane.

	$a^2 = 0.2m^2$			$a^2 = 0.4m^2$		
	$A^2m^2 = 1/54\times 4 = 0.004\,63$			$A^2m^2 = 1/54\times 4 = 0.004\,63$		
θ	q_R	q_S	q_K	q_R	q_S	q_K
0°	1.083	7.6	139.363	1.083	8.101	65.378
10°	1.083	7.587	143.951	1.083	8.065	67.703
45°	1.083	7.386	286.684	1.084	7.584	139.515
90°	1.084	7.193	∞	1.087	7.179	∞
135°	1.083	7.386	286.684	1.084	7.584	139.515
180°	1.083	7.6	139.363	1.083	8.101	65.378
	$A^2m^2 = 1/54 = 0.018\,52$			$A^2m^2 = 1/54 = 0.018\,52$		
0°	1.224	3.52	69.910	1.223	3.736	32.952
10°	1.224	3.513	72.210	1.224	3.719	34.119
45°	1.227	3.411	143.772	1.230	3.484	70.213
90°	1.231	3.314	∞	1.237	3.281	∞
135°	1.227	3.411	143.772	1.230	3.484	70.213
180°	1.224	3.52	69.910	1.223	3.736	32.952
	$A^2m^2 = 3/2\times 1/54 = 0.027\,78$			$A^2m^2 = 3/2\times 1/54 = 0.027\,78$		
0°	1.343	2.664	57.205	1.339	2.825	27.046
10°	1.344	2.658	59.086	1.341	2.811	28.003
45°	1.353	2.570	117.623	1.360	2.611	57.574
90°	1.365	2.483	∞	1.383	2.433	∞
135°	1.353	2.570	117.623	1.360	2.611	57.574
180°	1.343	2.664	57.205	1.339	2.825	27.046
	$A^2m^2 = 1/27 = 0.037\,04$			$A^2m^2 = 1/27 = 0.037\,04$		
0°	1.597	1.968	49.649	1.555	2.130	23.547
10°	1.6	1.967	51.281	1.561	2.113	24.378
42°	1.75	1.75	92.152	1.739	1.798	45.071
90°	*	*	∞	*	*	∞
138°	1.75	1.75	92.152	1.739	1.798	45.071
180°	1.597	1.968	49.649	1.555	2.130	23.547
	$A^2m^2 = 0.035\,74^\dagger$			$A^2m^2 = 0.034\,56^\dagger$		
0°	1.531	2.084	50.526	1.473	2.322	24.342
10°	1.534	2.077	52.187	1.476	2.307	25.201
45°	1.584	1.960	103.874	1.538	2.087	51.781
90°	1.736	1.736	∞	1.744	1.744	∞
135°	1.584	1.960	103.874	1.538	2.087	51.781
180°	1.531	2.084	50.526	1.473	2.322	24.342
	$a^2 = 0.8m^2$			$a^2 = m^2$		
	$A^2m^2 = 1/54\times 4 = 0.004\,63$			$A^2m^2 = 1/54\times 4 = 0.004\,63$		
0°	1.083	9.849	26.888	1.083	12.680	16.709
10°	1.083	9.960	28.203	1.083	11.806	18.501
45°	1.084	8.063	65.552	1.085	8.359	50.558
90°	1.086	7.151	∞	1.087	7.137	
135°	1.084	8.063	65.552	1.085	8.359	50.558
180°	1.083	9.849	26.888	1.083	12.680	17.709
	$A^2m^2 = \frac{1}{54} = 0.018\,52$			$A^2m^2 = \frac{1}{54} = 0.018\,52$		
0°	1.222	4.442	13.876	1.221	5.254	9.390
10°	1.223	4.372	14.525	1.222	5.055	10.054
45°	1.235	3.654	33.296	1.238	3.756	25.843
90°	1.250	3.217	∞	1.257	3.185	∞
135°	1.235	3.654	33.296	1.238	3.756	25.843
180°	1.222	4.442	13.826	1.221	5.254	9.390

	$a^2 = 0.8m^2$			$a^2 = m^2$		
	$A^2m^2 = \frac{3}{2}\times\frac{1}{54} = 0.027\,78$			$A^2m^2 = \frac{3}{2}\times\frac{1}{54} = 0.027\,78$		
θ	q_R	q_S	q_K	q_R	q_S	q_K
0°	1.333	3.325	11.554	1.329	3.824	8.059
10°	1.335	3.273	12.081	1.332	3.704	8.560
45°	1.372	2.709	27.467	1.378	2.767	21.404
90°	1.426	2.328	∞	1.450	2.273	∞
135°	1.372	2.709	27.467	1.378	2.767	21.404
180°	1.333	3.325	11.554	1.329	3.824	8.059
	$A^2m^2 = \frac{1}{27} = 0.037\,04$			$A^2m^2 = \frac{1}{27} = 0.037\,04$		
0°	1.507	2.539	10.195	1.490	2.880	7.272
10°	1.514	2.493	10.649	1.498	2.794	7.685
43°	1.806	1.806	22.262	1.798	1.861	17.358
90°	*	*	∞	*	*	∞
137°	1.806	1.806	22.262	1.798	1.861	17.358
180°	1.507	2.539	10.195	1.490	2.880	7.272
	$A^2m^2 = 0.032\,51^\dagger$			$A^2m^2 = 0.031\,61^\dagger$		
0°	1.408	2.906	10.784	1.386	3.401	7.691
10°	1.411	2.859	11.270	1.390	3.299	8.150
45°	1.486	2.319	25.522	1.468	2.436	20.181
90°	1.755	1.755	∞	1.760	1.760	∞
135°	1.486	2.319	25.522	1.468	2.436	20.181
180°	1.408	2.906	10.784	1.386	3.401	7.691
	$a^2 = 1.043\,09m^2$					
	$A^2m^2 = 1/54\times 4 = 0.004\,63$					
θ	q_R	q_S	q_K			
0°	1.083	*	*			
10°	1.083	13.248	15.812			
45°	1.085	8.429	48.059			
90°	1.087	7.134	∞			
135°	1.085	8.429	15.812			
180°	1.083	*	*			
	$A^2m^2 = 0.01$					
0°	1.137	9.580	9.580			
10°	1.137	8.188	11.670			
45°	1.142	5.553	33.165			
90°	1.148	4.697	∞			
135°	1.142	5.553	33.165			
180°	1.137	9.580	9.580			
	$A^2m^2 = \frac{3}{2}\times\frac{1}{54} = 0.027\,78$					
0°	1.329	4.002	7.386			
10°	1.331	3.845	7.908			
45°	1.380	2.780	20.397			
90°	1.456	2.260	∞			
135°	1.380	2.780	20.397			
180°	1.329	4.002	7.386			
	$A^2m^2 = \frac{1}{27} = 0.037\,04$					
0°	1.487	2.985	6.741			
10°	1.495	2.883	7.158			
43°	1.795	1.875	16.545			
90°	*	*	∞			
137°	1.795	1.875	16.545			
180°	1.487	2.985	6.741			

TABLE III. (*Continued.*)

		$a^2 = 1.04309m^2$ $A^2m^2 = 0.03142$†	
θ	q_R	q_S	q_K
0°	1.382	3.563	7.100
10°	1.385	3.433	7.573
45°	1.465	2.463	19.292
90°	1.761	1.761	∞
135°	1.465	2.463	19.292
180°	1.382	3.563	7.100

the Kerr solution there exist two surfaces r_i and r_0. The r_0 surface reduces to the Schwarzschild surface as the rotation is set equal to zero. The r_0 surface is similar to the surface produced by q_S. The q_S surface will be referred to as the Schwarzschild surface. The r_i surface is mainly a consequence of the rotation a. This surface is analogous to the surface produced by q_K. The q_K surface will be referred to as the Kerr surface. From the consideration of the static c-metric solution we saw that acceleration also produces two surfaces of infinite red-shift which are labeled r_S and r_R. The r_S surface is similar to the Schwarzschild surface q_S. The r_R surface was called the Rindler surface because it is mainly a consequence of the acceleration A and is similar to the q_R surface in the stationary c metric. The q_R surface will be called the Rindler surface. As to be expected from the Schwarzschild and c-metric solutions, we have three surfaces of infinite red-shift for the stationary c metric: the Rindler surface q_R, the Schwarzschild surface q_S, and the Kerr surface q_K.

In order to obtain the shapes of the surfaces of infinite red-shift in terms of the radial coordinate r and angular coordinate θ, notice that the radial coordinate r is related to the p and q coordinates by Eq. (2.9a). Substituting the values of p and q from Tables I and III into Eq. (2.9a), we obtain a relation between r and θ which gives the shapes of these surfaces expressed in the accelerating Boyer-Lindquist coordinate system. Table IV demonstrates this relation for different values of a and A. Surfaces denoted by r_R, r_S, and r_K in this table are the Rindler surface, the Schwarzschild surface, and the Kerr surface, respectively, and are respectively related to q_R, q_S, and q_K in Table III.

To investigate the dependence of these surfaces on the acceleration A and rotation a, let us first consider the special case of no rotation, i.e., $a=0$. It was shown that in the case of static c metric[3] the acceleration causes the Schwarzschild surface r_R to expand in the forward direction and contract in the backward direction. It was also shown in this case that by increasing the acceleration the Schwarzschild surface in the forward direction continues to expand further outward, while in the backward direction it first moves inward and then reverses its direction of motion and expands outward until, at the critical value $A=1/\sqrt{27}m$, the Schwarzschild surface and Rindler surface coincide in all points on their surfaces. In the presence of rotation the same qualitative type of behavior can be observed. Rotation acts to further distort these surfaces. Figure 2 shows the combined effect of the rotation, and the acceleration on the Schwarzschild surface r_S. Figure 2(a) shows the behavior of this surface under the change of the acceleration for a fixed value of rotation. The same kind of behavior as the nonrotating case can be observed in this figure. The Schwarzschild surface expands in the forward direction and shrinks in the backward direction. For larger accelerations this deformation is more significant. In the backward direction the surface moves back outward again for relatively large accelerations. As the acceleration is increased, the Rindler surface moves inward. Rotation causes the Rindler surface to contract slightly in the equatorial region.

As the acceleration is increased to a sufficiently large value, the Schwarzschild and Rindler surfaces will eventually coincide first on a ring in the equatorial plane for an acceleration slightly less than the nonrotating critical value $A=1/\sqrt{27}m$. It is in this situation that the discriminant Δ vanishes for $\theta=90$. As the acceleration continues to increase, the points of coincidence of the Schwarzschild and the Rindler surfaces spread out of the equatorial plane, towards the polar region. The points of coincidence of these two surfaces finally reach the poles for some value of the acceleration slightly larger than the nonrotating critical values.

Let us now consider the effect of acceleration on the Kerr surface. In the absence of acceleration this surface reduces to the interior Kerr surface which is symmetric about the equatorial plane. Acceleration distorts this symmetry and causes this surface to become elongated in the forward direction and contracted in the backward direction. This behavior of the Kerr surface under the change of the acceleration and the rotation is shown in Fig. 3. Figure 3(a) shows the behavior of this surface under the change of rotation for a fixed value of the acceleration. It can be seen in this figure that by increasing the rotation, the Kerr surface expands outward in all directions, except in the equatorial plane, as is the case for no acceleration. Figure 3(b) shows the behavior of the Kerr surface under the change of the ac-

TABLE IV. This table gives the relation between the radial coordinate r and the polar angle θ on the surfaces of infinite red-shift for different values of acceleration. Sections of this table that are marked by a dagger correspond to the case where the Schwarzschild and the Rindler surfaces coincide on a ring on the equatorial plane and the section marked by § corresponds to the case where the Schwarzschild and Kerr surfaces coincide on the poles.

	$a^2=0.2m^2$			$a^2=0.4m^2$		
	$A^2m^2=1/54\times4=0.00463$			$A^2m^2=1/54\times4=0.00463$		
θ	r_R/m	r_S/m	r_K/m	r_R/m	r_S/m	r_K/m
0°	∞	2.255	0.106	∞	2.094	0.229
10°	816.497	2.253	0.103	816.497	2.100	0.221
45°	43.611	2.213	0.051	43.482	2.149	0.106
90°	13.558	2.043	0	13.521	2.047	0
135°	8.351	1.823	0.051	8.346	1.779	0.105
180°	7.260	1.721	0.105	7.260	1.625	0.222
	$A^2m^2=\frac{1}{54}=0.01852$			$A^2m^2=\frac{1}{54}=0.01852$		
0°	∞	3.201	0.107	∞	2.924	0.232
10°	306.186	3.177	0.103	293.939	2.916	0.223
45°	17.250	2.816	0.051	17.169	2.740	0.106
90°	5.970	2.217	0	5.941	2.240	0
135°	3.911	1.809	0.051	3.905	1.777	0.104
180°	3.494	1.664	0.104	3.467	1.586	0.217
	$A^2m^2=\frac{3}{2}\times\frac{1}{54}=0.02778$			$A^2m^2=\frac{3}{2}\times\frac{1}{54}=0.02778$		
0°	∞	4.542	0.107	∞	4.038	0.233
10°	176.471	4.451	0.104	181.818	3.992	0.225
45°	11.561	3.456	0.051	11.450	3.380	0.106
90°	4.396	2.416	0	4.338	2.466	0
135°	3.008	1.868	0.051	2.996	1.844	0.103
180°	2.7	1.693	0.103	2.705	1.620	0.215
	$A^2m^2=\frac{1}{27}=0.03704$			$A^2m^2=\frac{1}{27}=0.03704$		
0°	∞	14.006	0.108	∞	9.037	0.236
10°	61.859	11.521	0.104	76.410	8.381	0.227
42°	6.337	6.337	0.057	6.455	6.014	0.118
90°	*	*	0	*	*	0
138°	2.153	2.153	0.056	2.162	2.111	0.114
180°	2.111	1.834	0.103	2.146	1.734	0.213
	$A^2m^2=0.03574^\dagger$			$A^2m^2=0.03456^\dagger$		
0°	∞	9.565	0.108	∞	6.336	0.235
10°	83.962	8.729	0.104	107.583	6.106	0.226
45°	7.347	4.826	0.051	7.969	4.395	0.106
90°	3.047	3.047	0	3.084	3.084	0
135°	2.383	2.038	0.051	2.473	1.975	0.103
180°	2.205	1.792	0.103	2.297	1.686	0.213
	$a^2=0.8m^2$			$a^2=m^2$		
	$A^2m^2=1/54\times4=0.00463$			$A^2m^2=1/54\times4=0.00463$		
θ	r_R/m	r_S/m	r_K/m	r_R/m	r_S/m	r_K/m
0°	∞	1.677	0.570	∞	1.267	0.941
10°	816.497	1.706	0.542	816.497	1.368	0.843
45°	43.611	2.009	0.227	43.482	1.931	0.295
90°	13.533	2.055	0	13.521	2.059	0
135°	8.346	1.682	0.222	8.341	1.626	0.287
180°	7.260	1.362	0.528	7.260	1.079	0.833

	$a^2=0.8m^2$			$a^2=m^2$		
	$A^2m^2=\frac{1}{54}=0.01852$			$A^2m^2=\frac{1}{54}=0.01852$		
θ	r_R/m	r_S/m	r_K/m	r_R/m	r_S/m	r_K/m
0°	∞	2.282	0.583	∞	1.822	0.900
10°	293.939	2.315	0.551	306.186	1.905	0.830
45°	17.050	2.578	0.226	17.010	2.491	0.294
90°	5.879	2.284	0	5.846	2.307	0
135°	3.892	1.706	0.216	3.885	1.667	0.277
180°	3.470	1.377	0.499	3.471	1.195	0.714
	$A^2m^2=\frac{3}{2}\times\frac{1}{54}=0.02778$			$A^2m^2=\frac{3}{2}\times\frac{1}{54}=0.02778$		
0°	∞	3.012	0.587	∞	2.405	0.892
10°	187.500	3.046	0.557	187.500	2.496	0.826
45°	11.299	3.212	0.225	11.215	3.119	0.292
90°	4.208	2.577	0	4.138	2.640	0
135°	2.976	1.789	0.213	2.967	1.759	0.272
180°	2.712	1.427	0.483	2.717	1.276	0.671
	$A^2m^2=\frac{1}{27}=0.03704$			$A^2m^2=\frac{1}{27}=0.03704$		
0°	∞	5.035	0.598	∞	3.738	0.899
10°	96.225	5.030	0.565	103.923	3.860	0.833
43°	5.871	5.871	0.243	5.952	5.551	0.316
90°	*	*	0	*	*	0
137°	2.111	2.111	0.227	2.117	2.064	0.288
180°	2.190	1.526	0.470	2.206	1.387	0.639
	$A^2m^2=0.03251^\dagger$			$A^2m^2=0.03161^\dagger$		
0°	∞	3.702	0.592	∞	2.791	0.892
10°	142.209	3.730	0.560	152.015	2.840	0.828
45°	8.874	3.804	0.225	9.251	3.569	0.291
90°	3.160	3.160	0	3.196	3.196	0
135°	2.609	1.874	0.220	2.667	1.828	0.270
180°	2.433	1.468	0.476	2.490	1.316	0.657

	$a^2=1.04309m^2$		
	$A^2m^2=1/54\times4=0.00463$		
θ	r_R/m	r_S/m	r_K/m
0°	∞	*	*
10°	816.497	1.207	0.997
45°	43.482	1.913	0.311
90°	13.521	2.060	0
135°	8.341	1.614	0.891
180°	7.260	*	*
	$A^2m^2=0.01^\S$		
0°	∞	1.184	1.184
10°	500.000	1.414	0.948
45°	27.027	2.092	0.309
90°	8.711	2.129	0
135°	5.533	1.608	0.296
180°	4.864	0.952	0.952

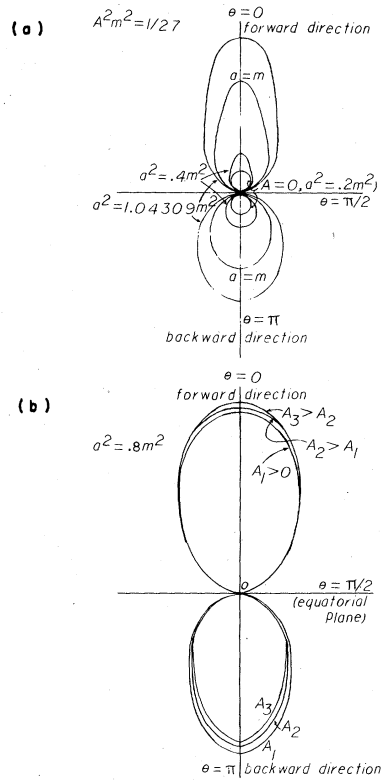

FIG. 2. The behavior of the Schwarzschild surface (a) under the change of the acceleration for a fixed value of rotation and (b) under the change of the rotation for a fixed value of acceleration is illustrated. The dotted surface in (a) is the Rindler surface when it coincides with the Schwarzschild surface on a ring on the equatorial plane and the discrete line is the Schwarzschild surface for the case when both a and A are equal to zero, which is spherically symmetric. The dotted surface in (b) is the Kerr surface when it coincides with the Schwarzschild surface on the poles.

celeration for a fixed and relatively small value of the rotation. As the acceleration increases, the Kerr surface becomes more deformed, shrinking in the backward direction and expanding in the forward direction. For large values of rotation, acceleration still causes the Kerr surface to expand in the forward direction and shrink in the backward direction. In addition, as the acceleration increases, the Kerr surface changes its direction of motion and it shrinks in the forward direction and expands in the backward direction. From Table IV one can see that the change of behavior discussed above occurs for the same value of rotation between $a^2=0.8m^2$ and $a^2=m^2$.

In the absence of acceleration, the Schwarzschild and the Kerr surfaces coincide at the poles for $a^2=m^2$. In the presence of the acceleration, a somewhat larger rotation is required to produce

TABLE IV. *(Continued.)*

	$a^2=1.043\,09m^2$ $A^2m^2=\frac{3}{2}\times\frac{1}{54}=0.027\,78$		
θ	r_R/m	r_S/m	r_K/m
0°	∞	2.245	0.991
10°	193.548	2.358	0.908
45°	11.194	3.099	0.307
90°	4.096	2.655	0
135°	2.964	1.752	0.285
180°	2.717	1.229	0.726
	$A^2m^2=\frac{1}{27}=0.037\,04$		
0°	∞	3.469	0.989
10°	103.923	3.613	0.910
43°	5.973	5.470	0.333
90°	*	*	0
137°	2.119	2.052	0.302
180°	2.209	1.350	0.683
	$A^2m^2=0.031\,42^\dagger$		
0°	∞	2.587	0.987
10°	156.709	2.707	0.906
45°	9.325	3.519	0.306
90°	3.204	3.204	0
135°	2.679	1.818	0.283
180°	2.502	1.272	0.708

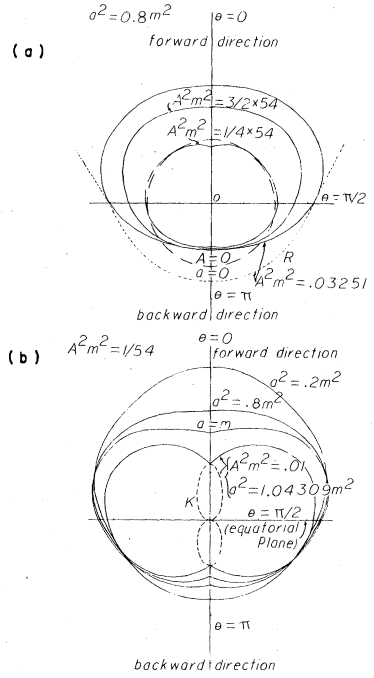

FIG. 3. This figure illustrates the behavior of the Kerr surface (a) under the change of the rotation for a fixed value of the acceleration and (b) under the change of the acceleration for a fixed and relatively small value of rotation. For larger rotations, although the acceleration causes the same kind of deformation, i.e., causing the Kerr surface to contract in the backward direction and expand in the forward direction, but by increasing the acceleration in this case, the deformation of the surface becomes *less* significant.

this coincidence because of the effects of the acceleration on these surfaces.

IV. CONCLUSIONS

The Schwarzschild metric, representing the gravitational field of a spherically symmetric and static particle, is known to have a spherically symmetric Killing horizon, which in this case coincides with the surface of infinite red-shift. Rotation and acceleration cause this spherically symmetric surface to distort. Rotation causes the Schwarzschild surface to contract along the poles, while rectilinear acceleration causes this surface to expand in the forward direction and contract in the backward direction.

In addition to the distorting effect of the Schwarzschild surface, acceleration and rotation introduce one more surface of infinite red-shift each. Therefore, a uniformly accelerating and rotating particle, in general, can have three surfaces of infinite red-shift. One is the Schwarzschild surface due to the mass which is being distorted by both acceleration and rotation, one due to the acceleration, and one due to the rotation of the particle.

ACKNOWLEDGMENT

This work was supported by National Aeronautics and Space Administration under Grant No. NSG-7639.

APPENDIX

Making the change of scale transformation

$$(\zeta,\eta,\sigma,\tau)\to l^{-1}(\zeta',\eta',\sigma',\tau'),$$
$$\gamma_0\to\gamma',\quad \epsilon_0\to l^2\epsilon',\quad m_0\to l^3m', \tag{A1}$$

where

$$l^{-2}=ab, \tag{A2}$$

followed by another change of scale

$$b\to\frac{1}{A},\quad \tau'\to\frac{\tau'}{A},\quad \sigma'\to\frac{-\omega}{A},\quad \zeta'\to -Ap,$$
$$\eta'\to -Aq,\quad P'\to A^2G,\quad Q'\to A^2F,\quad \gamma'\to A^2\gamma, \tag{A3}$$

followed by the coordinate transformation

$$t'=A(t-a\omega),$$

the line element (2.1) transforms to the line element (2.4).

[1]W. Kinnersley and M Walker, Phys. Rev. D 2, 1359 (1970).
[2]H. Farhoosh and R. L. Zimmerman, J. Math. Phys. 20, 2272 (1979).
[3]H. Farhoosh and R. L. Zimmerman, Phys. Rev D 21, 317 (1980).
[4]W. Kinnersley, J. Math. Phys. 10, 1195 (1969).
[5]J. F. Plebanski and M. Demianski, Ann. Phys. (N.Y.) 98, 98 (1976).
[6]Compare with the line element (2.1) of Ref. 3.
[7]See, for example, D. S. Meyler and O. G. Sutton, in *A Compendium of Mathematics and Physics* (English Universities Press, London, 1958).